NASA TECHNICAL MEMORANDUM

NASA TM X-3173

NASA TM X-3173

(NASA-TM-X-3173) SURFACE HEAT TRANSFER COEFFICIENTS OF PIN-FINNED CYLINDERS (NASA) 26 p HC $3.75 CSCL 20M

N75-14990

Unclas

H1/34 06991

SURFACE HEAT-TRANSFER COEFFICIENTS OF PIN-FINNED CYLINDERS

JAN 1975 RECEIVED NASA STI FACIL INPUT BRA

G. James Van Fossen, Jr.

Lewis Research Center and
U.S. Army Air Mobility R&D Laboratory
Cleveland, Ohio 44135

NATIONAL AERONAUTICS AND SPACE ADMINISTRATION • WASHINGTON, D. C. • JANUARY 1975

1. Report No.	2. Government Accession No.	3. Recipient's Catalog No.
NASA TM X-3173		

4. Title and Subtitle	5. Report Date
SURFACE HEAT-TRANSFER COEFFICIENTS OF PIN-FINNED CYLINDERS	January 1975
	6. Performing Organization Code

7. Author(s)	8. Performing Organization Report No.
G. James Van Fossen, Jr.	E-8125
	10. Work Unit No. 505-04

9. Performing Organization Name and Address	11. Contract or Grant No.
NASA Lewis Research Center and U.S. Army Air Mobility R&D Laboratory Cleveland, Ohio 44135	
	13. Type of Report and Period Covered Technical Memorandum

12. Sponsoring Agency Name and Address	14. Sponsoring Agency Code
National Aeronautics and Space Administration Washington, D.C. 20546	

15. Supplementary Notes

16. Abstract

An experimental investigation was conducted to measure heat-transfer coefficients for a 15.24-centimeter-diameter cylinder with pin fins on its surface. Pin diameters of 0.3175 and 0.6350 centimeter with staggered pin spacings of 3 and 4 pin diameters and pin lengths of 5, 7, and 9 pin diameters were tested. Flow was normal to the axis of the cylinder, and local heat-transfer coefficients were measured as a function of angle around the circumference of the cylinder. The average heat-transfer coefficient was also computed. Reynolds number based on pin diameter ranged from 3600 to 27 750. The smallest diameter, closest spacing, and largest pin-length-to-diameter ratio gave the highest average effective heat-transfer coefficients.

17. Key Words (Suggested by Author(s))	18. Distribution Statement
Pin fins Heat-transfer coefficient	Unclassified - unlimited STAR category 34 (rev.)

19. Security Classif. (of this report)	20. Security Classif. (of this page)	21. No. of Pages	22. Price*
Unclassified	Unclassified	25	$3.25

* For sale by the National Technical Information Service, Springfield, Virginia 22151

SURFACE HEAT-TRANSFER COEFFICIENTS OF PIN-FINNED CYLINDERS

by G. James Van Fossen, Jr.

Lewis Research Center and
U.S. Army Air Mobility R&D Laboratory

SUMMARY

An experimental investigation was conducted to measure heat-transfer coefficients for a 15.24-centimeter-diameter cylinder with pin fins on its surface. Pin diameters of 0.3175 and 0.6350 centimeter were tested. Pin spacings of 3 and 4 pin diameters and pin lengths of 5, 7, and 9 pin diameters were investigated. Flow was normal to the axis of the cylinder, and local heat-transfer coefficients were measured as a function of angle around the circumference of the cylinder. Average heat-transfer coefficients were then computed from the local heat-transfer coefficients. Reynolds numbers based on pin diameter ranged from 3600 to 27 750.

The pins were found to greatly increase the heat-transfer rate over that of a plain cylinder. The highest local heat-transfer coefficients were obtained at angles of 45° and 90° from the stagnation point. The lowest local heat-transfer coefficients were obtained at angles of 135° and 180°. The smallest diameter and closest spacing produced the highest average effective heat-transfer rate, and the largest pin-length-to-diameter ratio gave the highest average effective heat-transfer coefficient of those tested. The combination of pin diameters, spacings, and lengths tested were not sufficient to develop a general correlation.

INTRODUCTION

Convective heat-transfer coefficients were measured on a 15.24-centimeter-diameter cylinder with pin fins on its surface. Pin fins should maintain a high heat-transfer rate relative to annular fins when the flow direction is not normal to the axis of the cylinder. This property of pin fins can be an advantage when the flow direction is variable or uncertain. No heat-transfer data for pin fins on the surface of a single

cylinder are available in the open literature. The purpose of this report is to present measured heat-transfer coefficients for this case.

Heat-transfer coefficients were measured on the surface of a cylinder for five different pin fin geometries. In all five cases, airflow over the cylinder was normal to its axis. Heat-transfer coefficients were measured at five angular positions around the circumference of each cylinder. The angles were in 45° steps from 0° (facing directly upstream) to 180°. Average heat-transfer coefficients for the entire cylinder were computed from local data. The range of Reynolds number based on pin diameter was from 3600 to 27 750. A transient heating and cooling method was used to measure the heat-transfer coefficients. The maximum temperature of the cylinder was 411 K.

The work was done in the U.S. customary system of units. Conversion to the International System of Units (SI) was done for reporting purposes only.

TEST SPECIMENS

Heat-transfer coefficients were measured on five 15.24-centimeter-diameter cylinders with different staggered pin fin arrangements on the surface of each. The fin arrangement is shown in figure 1. Table I lists the relative pin spacings and pin lengths that were tested.

A segment of each cylinder about 7.62 centimeters high, 5.08 centimeters in arc length, and 1.27 centimeters thick was made of copper. Copper pin fins were silver soldered into holes drilled in the copper segment. An electric heater was silver soldered to the inside face of the segment. The heater consisted of a Nichrome V heater wire surrounded with an insulating layer of magnesium oxide which was held in place by a stainless-steel tube. Four Chromel-Alumel thermocouples were attached to the copper. The thermocouples were connected in parallel to read the average temperature of the segment. The copper segment was used as a calorimeter to measure heat-transfer coefficients.

The remaining portion of the cylinder was made of Micarta, which has a relatively low thermal conductivity, to minimize heat loss from the sides of the copper segment. In order to make the pin pattern continuous, steel pins were pressed into drilled holes around the circumference of the Micarta cylinder. Figure 2 shows the copper segment with the electric heater and the Micarta cylinder.

APPARATUS

The cylinder to be tested was mounted on a remotely controlled television camera positioner which allowed the cylinder to be rotated about its axis. The entire assembly

was attached to the floor of the Lewis Research Center's 9- by 15-Foot V/STOL Wind Tunnel (ref. 1). Figure 3 shows the assembly mounted in the tunnel. The angle of the copper calorimeter with respect to the flow direction was set visually by using a television monitor and the pointer and graduations shown in figure 3. Angles were accurate to about $\pm 2.5^{\circ}$.

Current was supplied to the electric heater through a variable transformer. This arrangement allowed the voltage across the heater to be varied from 0 to about 140 volts.

The single thermocouple lead wire from the measuring junction at the copper calorimeter was run to a reference oven whose temperature was 339 K. The voltage from the thermocouple was amplified 1000 times and was recorded as a function of time on an X-Y recorder during the test. At a later time an electronic digitizer coupled with a minicomputer was used to digitize the recorded data and to convert voltages to temperatures.

V/STOL tunnel control instrumentation was used to read the tunnel dynamic pressure and total temperature.

TEST PROCEDURE

Before each new cylinder was tested, the amplifier and X-Y recorder were calibrated. A known voltage from a precision potentiometer was fed to the amplifier whose output was connected to the X-Y recorder. The gain on the X-Y recorder was adjusted so the Y-displacement corresponded to the desired voltage reading.

The procedures for testing each of the five pin fin geometries were identical:

(1) The wind tunnel dynamic pressure was set to give the desired air speed in the test section.

(2) The angle of the copper calorimeter was set to the desired value.

(3) The X-Y recorder was started.

(4) The heater was switched on.

(5) When the predetermined maximum temperature was reached, the heater was switched off.

(6) The copper calorimeter was allowed to cool to a predetermined temperature.

(7) A new angle was set and steps 4, 5, and 6 were repeated.

(8) When all five angles (0° to 180° in 45° steps) were run, the air speed was changed and the procedure repeated.

THEORY

The objective of the test was to measure heat-transfer coefficients as a function of angle and air velocity for each of the five pin fin geometries. A transient technique, which involved heating and cooling of the copper calorimeter, was used to measure the heat-transfer coefficients. In order to calculate the desired heat-transfer coefficient from the transient temperature data of the copper calorimeter, a mathematical model of the calorimeter was needed. Several simplifying assumptions were made in order to develop such a model:

(1) The heat-transfer coefficient was assumed to be uniform over the entire surface of the copper calorimeter, that is, over the cylindrical surface, the pins, and the ends of the pins.

(2) The temperature of the cylindrical part of the calorimeter was assumed to be uniform; the only temperature gradient was in the pins.

(3) Heat loss from the calorimeter to the Micarta cylinder was negligible. (A finite difference model of the copper calorimeter and the Micarta cylinder showed the heat lost by conduction to be about 5 percent of the heat lost by convection for a low effective heat-transfer coefficient.)

(4) The thermal properties of the copper were assumed to be independent of temperature. With these assumptions, the copper calorimeter was divided into equal segments; one for each pin. A finite difference model for a single pin and the associated segment of base material was then taken as representative of the entire calorimeter. The thermal network used in the finite difference model for the 0.3175-centimeter-diameter pin with 3-diameter spacing and 9-diameter length is shown in figure 4.

The method of least squares was used to calculate the heat-transfer coefficient from the transient temperature data. The least-square function

$$F(h) = \sum_{i=1}^{N} \left[T_{exp,i} - T_{cal,i}^{(h)} \right]^2 \tag{1}$$

was minimized with respect to the heat-transfer coefficient h. The value of h that minimized F was assumed to be the true value. (All symbols are defined in the appendix.)

If the temperature of each node in the network at the time the heater was switched off were known, the heat-transfer coefficient could have been calculated from the cooling of the calorimeter only. However, only the temperature of the thermocouple location was known at that time. In any transient problem it is necessary to know the initial temperature of each node before a solution can be obtained. The temperature of each node of the calorimeter was known only before the heater was switched on. At that time the temperature of the fins was uniform. This made it necessary that the rate of heat

addition to the calorimeter be known. The rate of heat addition was not measured during the tests; only the voltage to the heater and its lead wires was measured. Because of uncertainty in the resistance of various elements in the heater circuit, it was not possible to accurately calculate the heating rate directly.

In reference 2 it is shown that, by using the method of least squares, it is possible to calculate both the heat-transfer coefficient and the heating rate simultaneously for a lumped-parameter calorimeter. A lumped-parameter calorimeter is essentially the same as the calorimeter used in these tests but with no pin fins. That is, it can be considered as a lump of material with no temperature gradients. For this case, equation (1) becomes

$$F(h, Q) = \sum_{i=1}^{N} \left[T_{exp,i} - T_{cal,i}(h, Q) \right]^2 \tag{2}$$

Reference 2 also defines optimum experimental conditions for the lumped-parameter calorimeter. The results obtained with this simple model were applied to the calorimeter used in these tests by defining an effective heat-transfer coefficient due to the presence of the pins. This was done by adding the heat convected out of the wall of the cylinder and the heat conducted through the base of the pin and equating this to the total heat loss based on an effective heat-transfer coefficient and the wall area. That is,

$$h_{eff} A_w (T_w - T_a) = h(A_w - A_p)(T_w - T_a) + Q_{pin} \tag{3}$$

The heat conducted through the base of the pin is given by (ref. 3)

$$Q_{pin} = \sqrt{PhA_p k_p}\,(T_w - T_a) \left[\frac{\sinh(m\ell) + \left(\frac{h}{mk_p}\right)\cosh(m\ell)}{\cosh(m\ell) + \left(\frac{h}{mk_p}\right)\sinh(m\ell)} \right] \tag{4}$$

where

$$m = \sqrt{\frac{hP}{k_p A_p}} \tag{5}$$

Substituting equation (4) into (3) and simplifying yields

$$h_{eff} = h\left[1 - \frac{\pi}{4\left(\frac{S}{D_o}\right)^2}\right] + \frac{\pi k_p m}{4\left(\frac{S}{D_o}\right)^2}\left[\frac{\sinh(m\ell) + \left(\frac{h}{mk_p}\right)\cosh(m\ell)}{\cosh(m\ell) + \left(\frac{h}{mk_p}\right)\sinh(m\ell)}\right] \tag{6}$$

The dimensionless heating rate parameter from reference 2 then becomes

$$\beta = \frac{Q}{h_{eff} A_w \Delta T_{max}} \tag{7}$$

and the dimensionless time is

$$\tau = \frac{h_{eff} t}{LC} \tag{8}$$

For this experiment a β of 1.04 was chosen. A β as close as possible to unity was shown to be the optimum in reference 2, but the real time for the experiment becomes very large for β approaching 1. From figure 8 in reference 2 the optimum dimensionless time τ_{opt} is 4.75 for a β of 1.04. For the calorimeters used in this experiment the characteristic length L was 1.27 centimeters and the heat capacity of copper was 3.4 J/(cm^3)(^{o}C). A representative value of h was 0.052 W/(cm^2)(^{o}C). Substituting these values into equation (7) and solving for the real time gave 394 seconds.

With β and τ_{opt} known the mathematical model of reference 2 was used to find the optimum temperature drop after the heater was switched off. With this information, it was much easier to tell when to stop taking data because h was unknown and dimensionless time could not be computed. For a β of 1.04 and a τ_{opt} of 4.75 the optimum dimensionless temperature was 0.225, or

$$\frac{T_w - T_a}{\Delta T_{max}} = 0.225 \tag{9}$$

The value of ΔT_{max} was chosen as 111 K, and the ambient temperature for most of the tests was 300 K. Substituting these temperatures into equation (9) and solving gave 325 K as the temperature at which the test could be terminated. The optimum procedure then

was to switch the heater on and allow the calorimeter to heat up to 411 K then switch the heater off and stop taking data when the temperature dropped below 325 K.

CALCULATION PROCEDURE

The heat-transfer coefficient h was calculated by minimizing equation (2) with respect to both h and Q. This was done by using the Gauss-Newton linearization method. Equation (2) was differentiated with respect to h and then Q to obtain

$$\frac{\partial F}{\partial h} = -2 \sum_{i=1}^{N} \left[T_{exp,i} - T_{cal,i}(h, Q) \right] \frac{\partial T_{cal,i}(h, Q)}{\partial h} \tag{10}$$

and

$$\frac{\partial F}{\partial Q} = -2 \sum_{i=1}^{N} \left[T_{exp,i} - T_{cal,i}(h, Q) \right] \frac{\partial T_{cal,i}(h, Q)}{\partial Q} \tag{11}$$

When F is at a minimum, equations (10) and (11) are zero. Let h^* and Q^* be the true values of h and Q (the values that minimize F) and h^0 and Q^0 be an initial guess of h and Q near h^* and Q^*. Expanding $T(h^*, Q^*)$ in a Taylor series about $T(h^0, Q^0)$ yields

$$T(h^*, Q^*) = T(h^0, Q^0) + \frac{\partial T}{\partial h} \Delta h + \frac{\partial T}{\partial Q} \Delta Q + \frac{\partial^2 T}{\partial h^2} \Delta h^2 + \frac{\partial^2 T}{\partial h \partial Q} \Delta h \Delta Q + \frac{\partial^2 T}{\partial Q^2} \Delta Q^2 + \ldots \tag{12}$$

Keeping only first-order terms, substituting equation (12) into equations (10) and (11), equating to zero, and solving for Δh and ΔQ gives

$$\Delta h = h^* - h^0 = \frac{\sum_i \left(\frac{\partial T}{\partial Q}\right)_i^2 \sum_i (T_{exp,i} - T_{cal,i}) \frac{\partial T}{\partial h} - \sum_i \left(\frac{\partial T}{\partial h}\right)_i \left(\frac{\partial T}{\partial Q}\right)_i \sum_i (T_{exp,i} - T_{cal,i}) \left(\frac{\partial T}{\partial Q}\right)_i}{\sum_i \left(\frac{\partial T}{\partial h}\right)_i^2 \sum_i \left(\frac{\partial T}{\partial Q}\right)_i^2 - \left[\sum_i \left(\frac{\partial T}{\partial h}\right)_i \left(\frac{\partial T}{\partial Q}\right)_i\right]^2} \tag{13}$$

$$\Delta Q = Q^* - Q^0 = \frac{\sum_i \left(\frac{\partial T}{\partial h}\right)_i^2 \sum_i (T_{exp,i} - T_{cal,i})_i \frac{\partial T}{\partial Q} - \sum_i \left(\frac{\partial T}{\partial h}\right)_i \left(\frac{\partial T}{\partial Q}\right)_i \sum_i (T_{exp,i} - T_{cal,i}) \left(\frac{\partial T}{\partial h}\right)_i}{\sum_i \left(\frac{\partial T}{\partial h}\right)_i^2 \sum \left(\frac{\partial T}{\partial Q}\right)_i^2 - \left[\sum_i \left(\frac{\partial T}{\partial h}\right)_i \left(\frac{\partial T}{\partial Q}\right)\right]^2} \tag{14}$$

The true values h^* and Q^* are usually not reached the first time, and so equations (13) and (14) are applied iteratively until

$$\frac{h^k - h^{k-1}}{h^k} < \delta \tag{15}$$

and

$$\frac{Q^k - Q^{k-1}}{Q^k} < \delta \tag{16}$$

where δ was taken as 0.001.

The partial derivatives in equations (13) and (14) were calculated numerically from the finite difference model. The numerical approximation used was

$$\left(\frac{\partial T}{\partial h}\right)_i \simeq \frac{T_{cal,i}(h + \delta h, Q) - T_{cal,i}(h, Q)}{\delta h} \tag{17}$$

and

$$\left(\frac{\partial T}{\partial Q}\right)_i \simeq \frac{T_{cal,i}(h, Q + \delta Q) - T_{cal,i}(h, Q)}{\delta Q} \tag{18}$$

where δ was again taken as 0.001.

The Gauss-Newton linearization method was found to be very efficient. Convergence was usually obtained in two or three iterations.

Reynolds number and Nusselt number were calculated based on the pin diameter. The viscosity and thermal conductivity of air used in the Reynolds number and Nusselt number, respectively, were evaluated at 311 K. The viscosity used was 1.912×10^{-5} N-sec/m^2 and the conductivity was 2.665×10^{-4} W/(cm)(^{o}C).

The average Nusselt number for each cylinder was also computed. In order to accomplish this calculation a power-law curve of the form

$$Nu_{D_o} = A\,Re_{D_o}^{B} \tag{19}$$

was fitted to the data for each of the five angles. The method of least squares was used to determine the coefficients A and B. Five Reynolds numbers that were representative of the points tested were chosen. For each Reynolds number the average Nusselt number for the five angles was computed from

$$\overline{Nu}_{D_o} = \frac{1}{5}\sum_{i=1}^{5} Nu_{D_o}(\theta_i) \tag{20}$$

A power-law curve was fitted to these five points to obtain a correlation for average Nusselt number as a function of Reynolds number for each cylinder.

The V/STOL tunnel test section density-velocity product was calculated from the tunnel dynamic pressure, the tunnel total pressure, and the tunnel static temperature as

$$\rho V = \sqrt{\frac{2q(P_t - q)}{RT_a}} \tag{21}$$

The total pressure was nearly identical to the barometric pressure, and the test section static temperature was approximately equal to the total temperature. The barometric pressure and the total temperature were used in equation (21).

RESULTS AND DISCUSSION

Figure 5 shows local Nusselt number as a function of Reynolds number with angle θ_i as a parameter for all five pin geometries. Average Nusselt number is also shown for each case. Table II gives Nusselt numbers and Reynolds numbers for individual test points. The coefficients A and B from equation (19) are also given in table II.

As expected, in all cases, both the 135^o and the 180^o angles have the lowest heat-transfer coefficients. The heat-transfer coefficients are lowest at 135^o because the flow around the cylinder has just separated at this angle and the velocity over the pins is probably near zero. The higher heat transfer coefficients at 180^o are probably due to

alternate vortex shedding by the cylinder, which would provide slightly higher alternating velocities in this region.

For the 0.635-centimeter-diameter pins the 45° and 90° angles have almost the same heat-transfer coefficients at any given Reynolds number. The 135° and 180° angles also have nearly the same heat-transfer coefficients. This change in the effect of angles on heat-transfer coefficient may be due to changes in the flow field caused by the increased ratio of pin diameter to cylinder diameter.

Figure 6 shows the average Nusselt number as a function of Reynolds number for all five pin geometries. The maximum spread in average Nusselt number is about 25 percent. Table III shows the coefficients A and B for each of the five pin geometries.

It is difficult to use figure 6 to compare the relative merits of each heat-transfer configuration because the Nusselt number uses pin diameter as a characteristic length. Also, the effect of total surface area has been removed from the heat-transfer coefficients. The best way to compare the heat-transfer characteristics of different pin geometries is to use equation (6) to compute an effective heat-transfer coefficient. This allows us to treat each configuration as simply a 15.24-centimeter-diameter cylinder with an effective heat-transfer coefficient on its surface. Figure 7 shows circumferentially averaged effective heat-transfer coefficients for the five pin geometries as a function of Reynolds number based on pin diameter.

It can be seen from figure 7 that the smallest diameter pins with the closest spacing gave the highest heat transfer. The best pin length was the one that gave the largest length-to-diameter ratio. This is to be expected since this configuration has the largest surface area of those tested. For a material with a lower thermal conductivity than copper, the increase in heat-transfer surface area obtained by using pins having greater length-to-diameter ratios than those tested may not increase the effective heat-transfer coefficient enough to justify the extra material used in the pins. In view of the simplifying assumption of uniform heat-transfer coefficient over the pin surface, care should be taken in applying these results when using pin materials whose conductivity varies significantly from that of copper.

The effect of pin diameter on the average effective heat-transfer coefficient can be seen by comparing the two cases that have 3-diameter spacings and 7-diameter lengths in figure 7. These two configurations have exactly the same surface area, but the larger diameter pins exhibit a lower effective heat-transfer coefficient. The lower effective heat-transfer coefficient for larger pins can be explained if we consider each pin as a cylinder in crossflow. For a cylinder, the larger the diameter, the smaller the average heat-transfer coefficient.

Also shown in figure 7 is the average heat-transfer coefficient for a 15.24-centimeter-diameter cylinder with no pins. This heat-transfer coefficient was calculated from (ref. 3, p. 411)

$$\frac{hD}{k_a} = 0.0239\ Re_D^{0.805} \tag{22}$$

The Reynolds number for the cylinder based on D was converted to that based on characteristic length D_o, by multiplying by the ratio of D_o to D, where D_o was taken as 0.3175 centimeter. This figure shows that pins greatly increase the heat-transfer rate from the cylinder.

SUMMARY OF RESULTS

The results of this experimental investigation to measure heat-transfer coefficients for a 15.24-centimeter-diameter cylinder with pin fins on its surface can be summarized as follows:

1. The highest local heat-transfer rates were obtained at 45° and 90° angles measured around the circumference of the cylinder.

2. The lowest local heat-transfer rates were obtained at 135° and 180° angles.

3. Based on average effective heat-transfer coefficient, the pins with the smallest diameter and closest spacing resulted in the highest heat-transfer rates. The longest pins for a given pin diameter gave the highest average effective heat-transfer coeffi-coefficients.

4. Not enough different pin diameters and spacings were tested to obtain a general correlation.

Lewis Research Center,
National Aeronautics and Space Administration,
and
U.S. Army Air Mobility R&D Laboratory,
Cleveland, Ohio,
505-04.

APPENDIX - SYMBOLS

A, B	coefficients used in power-law relation, eq. (19)
A_p	cross-sectional area of pin, m^2
A_s	surface area of node, m^2
A_w	surface area of cylinder associated with one pin, including the area covered by the pin, m^2
C	heat capacity of calorimeter, $J/(cm^3)(^oC)$
D	cylinder diameter, m
D_o	pin diameter, m
$F(h, Q)$	least-square function, defined by eq. (2)
h	average convective heat-transfer coefficient on surface of cylinder and pin, $W/(cm^2)(^oC)$
h_{eff}	effective heat-transfer coefficient due to presence of pins, defined by eq. (5), $W/(cm^2)(^oC)$
$\bar{h}_{eff}$	average effective heat-transfer coefficient, $W/(m^2)(^oC)$
k_a	thermal conductivity of air, $W/(cm)(^oC)$
k_p	thermal conductivity of pin material, $W/(cm)(^oC)$
L	characteristic dimension of lumped-parameter calorimeter, m
l	length of pin fin, m
m	pin fin parameter, defined by eq. (4)
N	number of data points
Nu_{D_o}	Nusselt number with pin diameter as characteristic length
$\overline{Nu}_{D_o}$	Nusselt number averaged around entire cylinder
P	perimeter of pin, m
P_t	tunnel total pressure, N/m^2
Q	heating rate, W
Q_{pin}	heat conducted through base of a pin fin, W
q	wind tunnel dynamic pressure, N/m^2
R	gas constant for air, $J/(gm)(^oC)$
Re_D	Reynolds number with cylinder diameter as characteristic length

Re_{D_o}	Reynolds number with pin diameter as characteristic length
S	pin spacing, m
T_a	air temperature, K
$T_{cal,i}(h, Q)$	temperature of calorimeter calculated from mathematical model at time t, K
$T_{exp,i}$	measured temperature of calorimeter at time t, K
T_w	surface temperature of cylinder, K
ΔT_{max}	maximum temperature rise above ambient, ^oC
t	time, sec
β	dimensionless heating rate
δ	arbitrary small number
θ_i	angle of calorimeter with respect to upstream flow direction
τ	dimensionless time, defined by eq. (7)
τ_{opt}	optimum dimensionless time, from ref. 2

REFERENCES

1. Yuska, J. A.; Diedrich, J. H.; and Clough, N.: Lewis 9- by 15-Foot V/STOL Wind Tunnel. NASA TM X-2305, 1971.
2. Van Fossen, G. James, Jr.: Design of Experiments for Measuring Heat-Transfer Coefficients with a Lumped-Parameter Calorimeter. NASA TN D-7857, 1974.
3. Kreith, Frank: Principles of Heat Transfer. International Textbook Co., 1966.

TABLE I. - PIN FIN GEOMETRIES

TESTED

Pin diameter, D_o, cm	Pin spacing-to-diameter ratio, S/D_o	Pin length-to-diameter ratio, l/D_o
0.3175	3	5
↓	3	7
	3	9
	4	7
.6350	3	7

TABLE II. - NUSSELT AND REYNOLDS NUMBERS BASED ON PIN DIAMETER FOR INDIVIDUAL TEST POINTS

(a) Pin diameter, D_o, 0.3175 cm; pin spacing-to-diameter ratio, S/D_o, 3; pin length-to-diameter ratio, ℓ/D_o, 9

Reynolds number with pin diameter as characteristic length, Re_{D_o}	Nusselt number with pin diameter as characteristic length, Nu_{D_o}
Angle of calorimeter, θ_i, 0°; A = 0.2239; B = 0.5173	
4 776.2	18.7
5 960.1	20.3
5 960.1	20.9
8 384.7	25.7
11 741.8	28.3
4 597.8	18.2
8 409.0	23.4
8 376.5	23.3
10 209.2	25.8
Angle of calorimeter, θ_i, 45°; A = 0.1842; B = 0.5929	
5 960.1	32.1
8 360.3	38.5
11 717.4	49.9
8 400.9	39.1
8 376.5	40.3
10 209.2	42.9
10 184.8	41.7
Angle of calorimeter, θ_i, 90°; A = 0.3731; B = 0.4836	
4 760.0	22.1
5 968.2	25.6
8 368.4	29.4
11 709.3	33.1
Angle of calorimeter, θ_i, 90°; A = 0.3731; B = 0.4836	
11 701.2	35.4
8 400.9	28.5
10 201.1	32.8
10 184.8	33.4
Angle of calorimeter, θ_i, 135°; A = 0.1010; B = 0.5578	
4 776.2	11.2
5 976.3	13.2
8 368.4	15.2
11 701.2	19.6
8 392.8	16.3
10 201.1	17.2
10 184.8	16.4
Angle of calorimeter, θ_i, 180°; A = 0.2786; B = 0.4708	
4 768.1	14.8
5 968.2	17.0
8 368.4	19.3
11 685.0	22.2
8 384.7	19.7
10 192.9	22.3
10 192.9	21.4

TABLE II. - Continued. NUSSELT AND REYNOLDS NUMBERS BASED ON PIN DIAMETER FOR INDIVIDUAL TEST POINTS

(b) Pin diameter, D_o, 0.3175 cm; pin spacing-to-diameter ratio, S/D_o, 3; pin length-to-diameter ratio, l/D_o, 7

Reynolds number with pin diameter as characteristic length, Re_{D_o}	Nusselt number with pin diameter as characteristic length, Nu_{D_o}
Angle of calorimeter, θ_i, 0°; A = 0.1748; B = 0.5217	
8 490.1	19.1
8 465.7	20.5
8 449.5	19.5
10 298.4	22.0
10 322.7	21.9
11 855.3	22.5
11 831.0	23.8
11 814.7	22.5
13 160.8	25.0
4 558.0	13.6
4 008.3	13.6
Angle of calorimeter, θ_i, 45°; A = 0.0898; B = 0.6501	
4 431.5	21.2
8 392.8	32.1
8 465.7	30.7
8 449.5	31.8
10 290.3	35.2
10 322.7	38.8
13 185.2	42.2
4 379.6	21.4
13 290.8	45.9
Angle of calorimeter, θ_i, 90°; A = 0.0949; B = 0.6061	
4 431.5	16.0
8 392.8	20.4
8 506.3	22.1
Angle of calorimeter, θ_i, 90°; A = 0.0949; B = 0.6061	
10 290.3	24.2
10 322.7	27.4
13 314.9	32.0
3 995.3	14.8
13 306.8	30.5
Angle of calorimeter, θ_i, 135°; A = 0.0914; B = 0.5505	
4 431.5	9.1
8 409.0	13.2
8 546.8	13.2
10 347.0	16.8
10 347.0	13.8
10 330.8	14.3
13 387.9	17.0
4 121.8	9.1
Angle of calorimeter, θ_i, 180°; A = 0.2169; B = 0.4724	
5 643.8	13.2
4 433.2	11.5
8 417.1	15.1
8 457.6	15.3
10 338.9	17.3
10 322.7	16.6
13 379.8	19.8

TABLE II. - Continued. NUSSELT AND REYNOLDS NUMBERS BASED ON PIN DIAMETER FOR INDIVIDUAL TEST POINTS

(c) Pin diameter, D_o, 0.3175 cm; pin spacing-to-diameter ratio, S/D_o, 3; pin length-to-diameter ratio, l/D_o, 5

Reynolds number with pin diameter as characteristic length, Re_{D_o}	Nusselt number with pin diameter as characteristic length, Nu_{D_o}	Reynolds number with pin diameter as characteristic length, Re_{D_o}	Nusselt number with pin diameter as characteristic length, Nu_{D_o}
Angle of calorimeter, θ_i, 0°; A = 0.1434; B = 0.5418		Angle of calorimeter, θ_i, 90°; A = 0.1615; B = 0.5425	
3 597.9	12.4	4 438.8	15.5
6 001.4	15.2	6 005.5	18.0
8 490.1	19.6	8 482.0	21.7
11 822.8	23.3	11 863.4	26.4
		13 728.5	28.3
Angle of calorimeter, θ_i, 45°; A = 0.1335; B = 0.6093		Angle of calorimeter, θ_i, 135°; A = 0.0857; B = 0.5622	
4 440.5	22.0		
3 598.8	20.1	6 751.5	12.2
6 005.5	26.1	8 473.9	13.8
8 482.0	33.2	11 806.6	16.7
11 855.3	39.5		
13 752.8	45.7	Angle of calorimeter, θ_i, 180°; A = 0.1547; B = 0.5167	
		6 749.1	14.7
		8 473.9	16.7
		11 798.5	19.6

TABLE II. - Continued. NUSSELT AND REYNOLDS NUMBERS BASED ON PIN DIAMETER FOR INDIVIDUAL TEST POINTS

(d) Pin diameter, D_o, 0.3175 cm; pin spacing-to-diameter ratio, S/D_o, 4; pin length-to-diameter ratio, l/D_o, 7

Reynolds number with pin diameter as characteristic length, Re_{D_o}	Nusselt number with pin diameter as characteristic length, Nu_{D_o}
Angle of calorimeter, θ_i, 0°; A = 0.1481; B = 0.5322	
5 327.6	14.2
5 278.9	13.4
5 935.8	14.3
8 384.7	18.4
8 473.9	18.7
8 457.8	19.0
13 839.3	23.5
13 777.1	23.0
4 736.4	14.2
10 184.8	19.5
10 225.4	20.8
Angle of calorimeter, θ_i, 45°; A = 0.1113; B = 0.6301	
5 295.1	24.6
5 943.9	26.1
8 392.8	33.0
8 465.7	33.3
8 457.6	34.6
11 733.6	41.1
13 533.8	44.1
13 647.4	46.9
13 752.8	43.8
5 059.2	23.2
10 176.7	36.4
10 225.4	37.0
4 388.6	22.7
Angle of calorimeter, θ_i, 90°; A = 0.1318; B = 0.5910	
5 351.9	20.9
5 943.9	21.6
8 392.8	28.4
8 465.7	27.2
8 457.6	28.3
Angle of calorimeter, θ_i, 90°; A = 0.1318; B = 0.5910	
13 558.2	36.4
13 598.7	36.5
13 736.6	36.3
5 065.7	20.7
10 176.7	31.0
10 217.3	30.5
Angle of calorimeter, θ_i, 135°; A = 0.1268; B = 0.5219	
5 384.3	11.4
5 943.9	12.0
8 384.7	14.4
8 465.7	14.3
8 457.6	13.9
13 582.5	16.7
13 614.9	17.9
13 769.0	20.7
5 081.9	10.7
10 184.8	15.5
10 217.3	15.4
Angle of calorimeter, θ_i, 180°; A = 0.1461; B = 0.5187	
5 384.3	12.7
5 943.9	13.0
8 376.5	16.3
8 465.7	15.6
13 631.1	26.7
13 623.0	18.8
13 769.0	20.2
5 084.3	11.9
8 384.7	15.6
10 192.9	18.5
10 209.2	18.6

TABLE II. - Concluded. NUSSELT AND REYNOLDS NUMBERS BASED ON PIN DIAMETER FOR INDIVIDUAL TEST POINTS

(e) Pin diameter, D_o, 0.6350 cm; pin spacing-to-diameter ratio, S/D_o, 3; pin length-to-diameter ratio, l/D_o, 7

Reynolds number with pin diameter as characteristic length, Re_{D_o}	Nusselt number with pin diameter as characteristic length, Nu_{D_o}
Angle of calorimeter, θ_i, 0°; A = 0.2468; B = 0.5025	
9 033.9	24.3
12 110.6	27.2
17 117.9	34.1
17 085.5	32.5
27 670.7	41.6
27 654.5	42.5
Angle of calorimeter, θ_i, 45°; A = 0.1611; B = 0.5978	
9 033.9	38.6
12 110.6	43.7
17 117.9	52.7
17 101.7	54.0
27 703.1	77.4
27 638.2	70.9
Angle of calorimeter, θ_i, 90°; A = 0.1271; B = 0.6267	
9 032.3	38.4
12 076.5	45.2
17 134.1	57.8
Angle of calorimeter, θ_i, 90°; A = 0.1271; B = 0.6267	
17 101.7	57.7
27 719.3	79.1
27 605.8	74.9
Angle of calorimeter, θ_i, 135°; A = 0.1127; B = 0.5583	
9 051.7	18.2
12 061.9	22.0
17 134.1	25.6
17 085.5	25.3
27 751.7	33.7
27 524.8	35.0
Angle of calorimeter, θ_i, 180°; A = 0.0817; B = 0.5926	
9 192.8	18.0
12 016.8	21.7
17 150.3	27.1
17 085.5	25.8
27 767.9	34.4
27 492.4	35.4

TABLE III. - POWER LAW COEFFICIENTS FOR AVERAGE NUSSELT NUMBER AS FUNCTION OF REYNOLDS NUMBER

$\left[\overline{Nu}_{D_o} = A\, Re_{D_o}^{B}.\right]$

Pin diameter, D_o, cm	Pin spacing-to-diameter ratio, S/D_o	Pin length-to-diameter ratio, ℓ/D_o	A	B
0.3175	3	9	0.21	0.53
	3	7	.11	.58
	3	5	.13	.56
	4	7	.10	.60
.6350	3	7	.13	.58

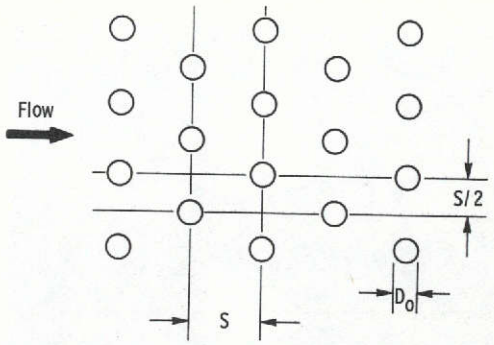

Figure 1. - Pin fin arrangement.

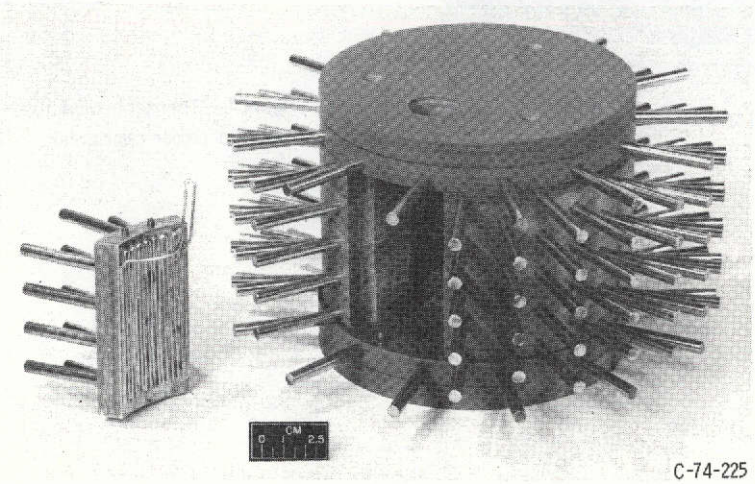

Figure 2. - Copper test segment with electric heater and Micarta cylinder.

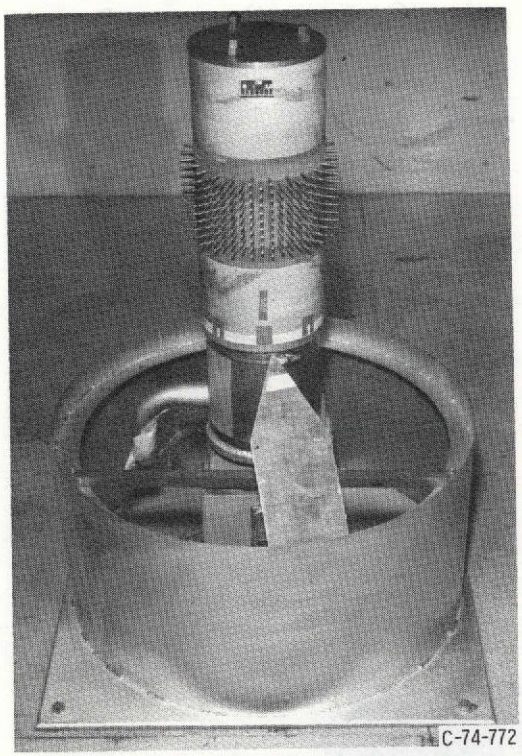

Figure 3. - Pin-finned cylinder installed in V/ STOL tunnel

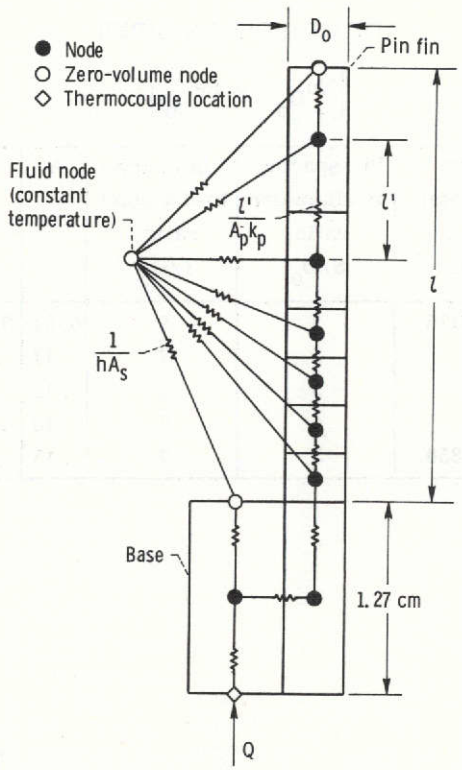

Figure 4. - Thermal network used in finite difference model of copper calorimeter.

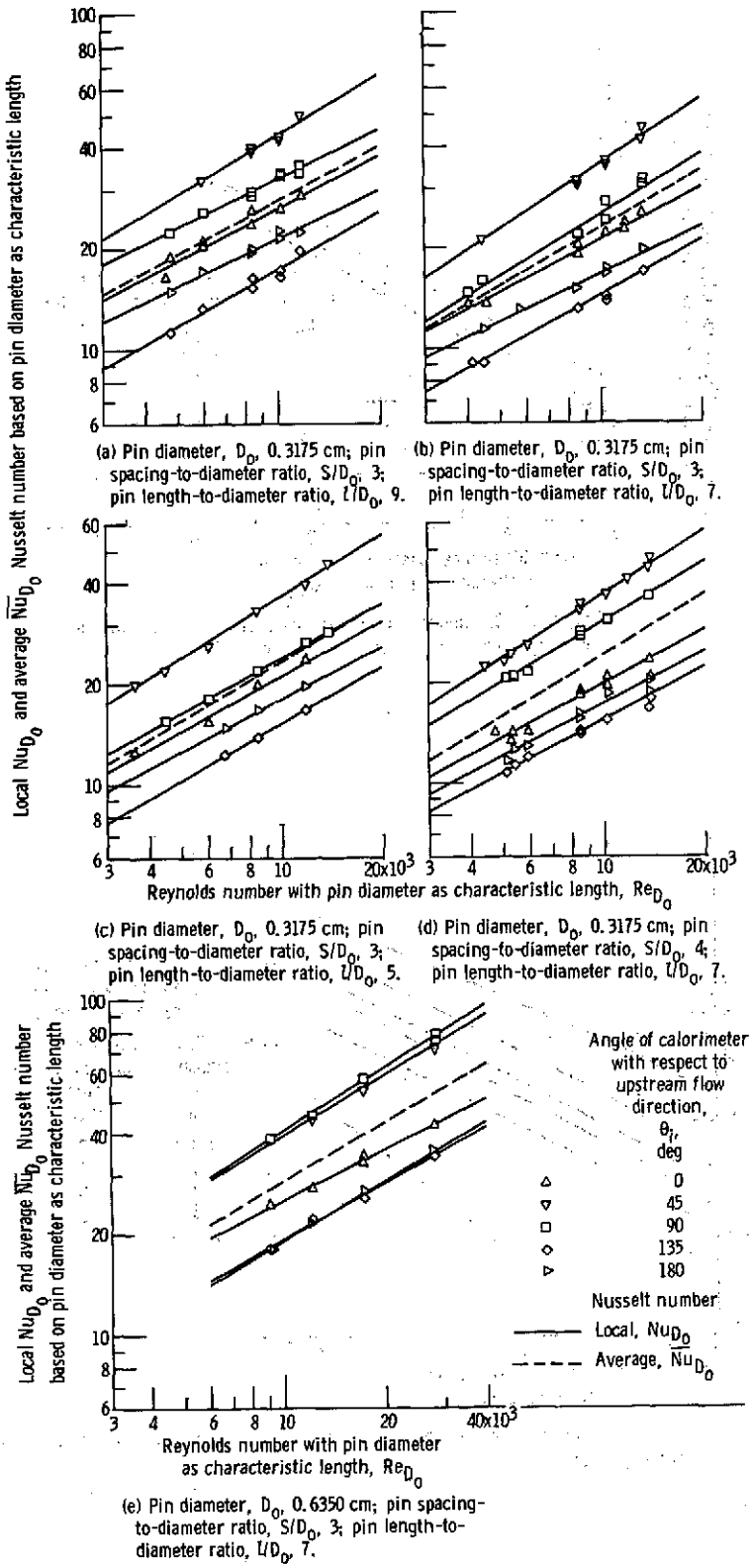

Figure 5. - Local and circumferentially averaged Nusselt number variation with Reynolds number and the angle of the calorimeter for all five pin geometries.

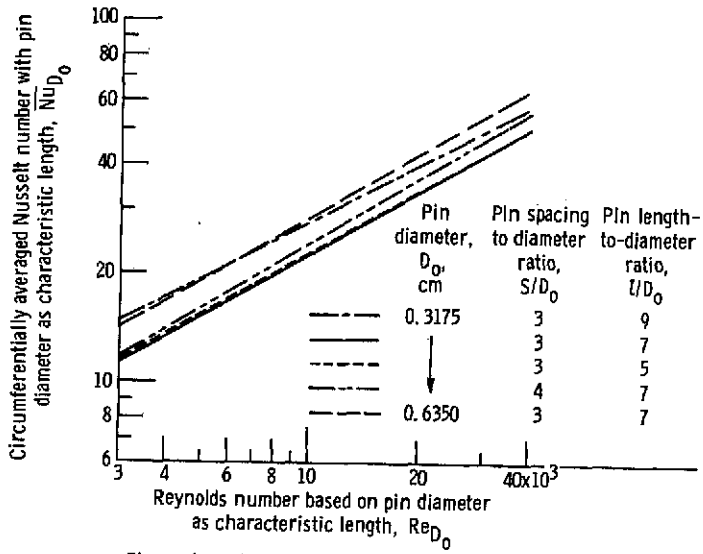

Figure 6. - Circumferentially averaged Nusselt number variation with Reynolds number for all five pin geometries.

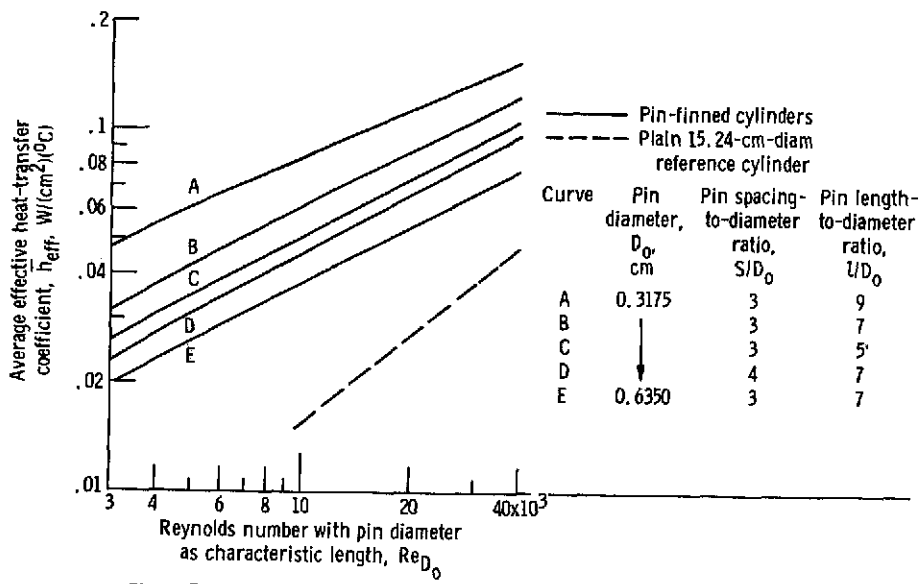

Figure 7. - Average effective heat-transfer coefficient variation with Reynolds number for each cylinder.